Naskar I, et al., J Pulm Med Respir Res 2023, 9: 079
DOI: 10.24966/PMRR-0177/100079

HERALD

Journal of Pulmonary Medicine and Respiratory Research

Research Article

Variable Clustered Fuzzy Rules for Self-Tuning Scheme for Respiratory Distresses by Similarity and the Phase Plane Trajectory Concept

Indrajit Naskar*, A.K. Pal and Nandan Kumar Jana

Department of Applied Electronics and Instrumentation Engineering, Heritage Institute of Technology, Kolkata, India.

Abstract

This work proposes a fuzzy rule extraction methodology for a self-tuning fuzzy controller based on the fuzzy clustering method (FCM) and the similarity approach technique. The similarity technique and phase plane trajectory method are used to even lower the acquired rules. To show a potential rule extraction scheme, the self-tuning fuzzy-logic-based proportional-derivative (STFLPDC) with 49 expert fuzzy rules and 49 clustered fuzzy gain rules is used. The utility of the approach is validated using common clustering validity indices. With 49 initial clustered fuzzy rules, the suggested method addressed oxygen supply in a human respiratory model. After further reduction using the similarity strategy, 29 and 14 fuzzy rules remained. Parallel to this, a real-time benchmark application using 49, 21, and 16 extracted fuzzy gain rules is used to access the performance of a lab-based overhead crane. Finally, to investigate control performance in both models, the phase plane trajectory concept is used to generate as few as 13 fuzzy gain rules.

Keywords: Fuzzy Clustering Method; Fuzzy Logic Based Proportional Plus Derivative Controller; Human Respiratory Model; Overhead Crane Model; Phase Plane Trajectory Method; Similarity Approach; Self-Tuning

Introduction

The knowledge-based fuzzy logic design is a widely used method in engineering fields like process automation and control; and non-engineering fields like economics, prediction of human behavior, and others [1]. Rule development is an important component in fuzzy model the building process; it depends on skilled expertise [2,3] A data-driven simplified self-extracted and reduced rule-base method is demonstrated in this work in order to develop a through computation powerful and linguistically comprehensible fuzzy scheme for self-tuning fuzzy logic-based PD controllers (STFLPDCs), overcoming its dependence on the expert-based rule for the tuning process.

The Fuzzy C-Means (FCM) based clustering algorithm could be used to determine the membership values of the data points with the pre-defined number of clusters [4,5], and the similarity approach concept is applied to generate a meaningful fuzzy rule base from the cluster data that are logically overlapping [6-8]. The overlapped and similar rules were reduced by implementing the similarity approach with some pre-defined limiting conditions. The extracted rules are shrunk further through the phase plane trajectory approach, which states that rules are only accountable for error and the change of error to zero (tends to zero). The presented scheme is validated by partition coefficient (PE), partition entropy (PC), Xie and Beni (XB), etc. [9,10].

Rule Extraction by FCM and Similarity Approach

In expert rule base guidance for designing the self-tuning fuzzy controllers where the development of the fuzzy if-then rule is one of the critical tasks compared to other parts of the design under consideration. Any particular algorithm or standard method not yet established to extract some meaningful if-then rules from any processes [11,12]. Automatic efficient rule extraction and also rule reduction techniques (similarity and phase plane trajectory) are presented to extract fuzzy rules from the process data in order to address the issues of dependence on skilled professionals and the system in question itself. The developed human respiratory model and the crane model (Make: FEEDBACK, UK) are used to further examine the acquired fuzzy rule basis for STFLPDCs. The FCM algorithm initially clusters the data into seven specified fuzzy regions, after which (49) rules are extracted and also reduced to distinct numbers that correspond to the similarity analysis procedure. The phase plane trajectory approach further reduces these derived (49) rules to 13 rules. Algorithm: Extracting and reducing data-driven rules:

1. In this work, error (e_k), change of error (Δe_k), and gain (β_k), are inputs and output, where $k = 1, \ldots, N$; the number of data, N=1001.

2. $v_e = [v_{e1}, v_{e2} \ldots v_{ei}]$, $v_{\Delta e} = [v_{\Delta e1}, v_{\Delta e2} \ldots v_{\Delta ei}]$, and $v_\beta = [v_{\beta 1}, v_{\beta 2} \ldots v_{\beta i}]$ are initial cluster center for inputs and output, where, $i = 1, \ldots, c$, $(2 \leq c \leq N)$, and $c = 7$.

Set a threshold value (ε) to stop the iteration.

3. Now, $\mu_{ik}(e_k)$, $\mu_{ik}(\Delta e_k)$, and $\mu_{ik}(\beta_k)$ are initial fuzzy membership function with size $c * N$.

4. Cluster centers are updated by equation (1) with $m = 2$, $(1 < m < \infty)$,

$$v_i = \frac{\sum_{k=1}^{N} (\mu_{ik})^m x_k}{\sum_{k=1}^{N} (\mu_{ik})^m} \quad (1)$$

5. The equation (2) is used to update the membership functions.

$$\mu_{ik} = \left[\sum_{j=1}^{c} \left(\frac{(d_{ik})}{(d_{jk})}\right)^{\frac{2}{m-1}}\right]^{-1} \quad (2)$$

***Corresponding author:** Indrajit Naskar, Heritage Institute of Technology, Kolkata, India. Email: Indrajit.naskar@heritageit.edu

Citation: Naskar I, Pal AK, Jana NK (2023) Variable Clustered Fuzzy Rules for Self-Tuning Scheme for Respiratory Distresses by Similarity and the Phase Plane Trajectory Concept. J Pulm Med Respir Res 9: 079.

Received: May 19, 2023; **Accepted:** June 6, 2023; **Published:** June 12, 2023

Where, $d_{ik} = [\sum_{i=1}^{c}(x_k - v_i)^2)]^{\frac{1}{2}}$, and d_{ik} is calculated with the concept of Euclidean distance from the kth point of any input data to last updated centers as in step 4.

$d_{jk}=[\sum_{j=1}^{c}(x_k - v_j)^2)]^{1/2}$,

d_{jk} is the Euclidean distance from the kth point of any input data set to the initial cluster centers. Where, 'j' is a variable on the coordinate space and $j = 1, \dots, c$.

6. Here, 'N' data points are partitioned by FCM into predefined 'c' region using the following condition should be minimum.

The objective function:

$$J_{min} = \sum_{k=1}^{N}\sum_{i=1}^{c}(\mu_{ik})^m \|x_k - v_i\|^2 \qquad (3)$$

7. Keep carrying out steps 4 through 6 until the halting criterion is met and the condition is satisfied. $\sum_{k=1}^{N}\mu_{ik} = 1$

8. Choose a single cluster of data that has the highest membership function value, and then is set up it according to order of ascending.

9. Update centers (v_{e1}, $v_{\Delta e1}$,) using cluster data from step 8 and sorting based on the corresponding membership value developed from step 8 using equation (1).

10. $d_{ik} = [\sum_{i=1}^{c}(\beta_k - v_{e1})^2)]^{1/2}$, is evaluated with the kth output of gain (β_k) from step 8 to 1st updated center of (v_{e1}) from step 9, and make them sorted. Repeat the process for $v_{\Delta e1}$.

11. If $d_{ik}>$ limiting value, perform $e_k \cap \beta_k$, and $\Delta e_k \cap \beta_k$. Updated the centers and MFs values as per equations (1) and (2) by the condition, $d_{ik}>$ limiting value. Overlapping data of (e_k, Δe_k) with βk are calculated by $e_k \cap \beta_k$, and $\Delta e_k \cap \beta_k$. Now, updated fuzzy regions are expressed as

$v_{e1\beta i} = [v_{e1\beta 1}, v_{e1\beta 2} \cdots v_{e1\beta i}]$, and

$v_{\Delta e1\beta i} = [v_{\Delta e1\beta 1}, v_{\Delta e1\beta 2} \cdots v_{\Delta e1\beta i}]$ for the first set of data as arranged in step 8.

12. Repeat steps 10 and 11 for other centers of error and change of error centers with output.

$$\begin{bmatrix} v_{e2\beta i} = [v_{e2\beta 1}, v_{e2\beta 2} \cdots v_{e2\beta i}] \\ \vdots \\ v_{e7\beta i} = [v_{e7\beta 1}, v_{e7\beta 2} \cdots v_{e7\beta i}] \end{bmatrix}$$

and

$$\begin{bmatrix} v_{\Delta e2\beta i} = [v_{\Delta e2\beta 1}, v_{\Delta e2\beta 2} \cdots v_{\Delta e2\beta i}] \\ \vdots \\ v_{\Delta e7\beta i} = [v_{\Delta e7\beta 1}, v_{\Delta e7\beta 2} \cdots v_{\Delta e7\beta i}] \end{bmatrix}$$

13. Now the complete rules due to ($v_{ei\beta i}$) and ($v_{\Delta ei\beta i}$) are expressed as

$$\begin{bmatrix} v_{e1\beta 1}, v_{e1\beta 2} \cdots v_{e1\beta 7} \\ v_{e2\beta 1}, v_{e2\beta 2} \cdots v_{e2\beta 7} \\ \vdots \\ v_{e7\beta 1}, v_{e7\beta 2} \cdots v_{e7\beta 7} \end{bmatrix}$$

And $\begin{bmatrix} v_{\Delta e1\beta 1}, v_{\Delta e1\beta 2} \cdots v_{\Delta e1\beta 7} \\ v_{\Delta e2\beta 1}, v_{\Delta e2\beta 2} \cdots v_{\Delta e2\beta 7} \\ \vdots \\ v_{\Delta e7\beta 1}, v_{\Delta e7\beta 2} \cdots v_{\Delta e7\beta 7} \end{bmatrix}$

14. Combined the extracted rules either by max or min operation to generate 49 extracted rules as follows. $v_{ei\beta i} \cup v_{\Delta ei\beta i}$, or $v_{ei\beta i} \cap v_{\Delta ei\beta i}$

The rules are automatically extracted to generate 29/14 rules for the respiratory and also 21/16 from the 49 extracted rules for the crane by simply altering the inter-cluster distance limiting criterion in the similarity approach and repeating steps 10 through 14.

FCM Cluster Validity Check by Different Indices

The various validity indices are applied to judge the results of the selected clustering method that best fits the partitioning of the data [9,10,13] High compactness and low separation values are the ideal parameters to validate in the context of FCM.

Bezdek [10] derived the partition coefficient (V_{PC}) and partition entropy (V_{PE}),

$$V_{PC} = \frac{1}{N}\sum_{i=1}^{c}\sum_{j=1}^{N}\mu_{ij}^2 \text{ and } V_{PE} = -\frac{1}{N}\sum_{i=1}^{c}\sum_{j=1}^{N}\mu_{ij} log_a^{\mu_{ij}} \qquad (4)$$

The high PC value is good (closer to unity) and the low value of PE to '0' is better.

In Xie and Beni's [9] index V_{XB}, a low value of V_{XB} justifies good clustering.

$$V_{XB} = \frac{\sum_{i=1}^{c}\sum_{j=1}^{N}\mu_{ij}^m\|x_j - v_i\|^2}{N*(min_{i\neq j}\|v_i - v_j\|^2)} \qquad (5)$$

Silhouette Coefficient (SC), a high value (≤1) is a good indicator [13].

$$sc = \begin{cases} 1-\frac{a}{b}, & if\ a<b \\ 0, & if\ a=b \\ \frac{b}{a}-1, & if\ a>b \end{cases} \qquad (6)$$

As per Dunn Index (DI) [13],

$$DI = min_{1\le i\ll c}\left\{min_{1\ll j\ll c, i\neq j}\left\{\frac{\delta(x_i,x_j)}{max_{i\ll k\ll c}\Delta(x_k)}\right\}\right\} \qquad (7)$$

Phase Plane Trajectory-Based Rule Reduction

The process response and its associated phase plane trajectory are shown in figures. 1a-1b and Table 1, where the error (e) is zero at "b_1" and "b_3", the change of error (Δe) is zero at "b_2" and "b_4", and both are zero at "c" [14,15]. By only selecting the rules where (e, Δe) are approaching zero, as illustrated in Tables 2 & 3, the extracted 49 rules are then reduced to 13. Phase plane trajectory tracing for an overhead crane with the different rules are shown in figure. 2, depicting stable and converged responses.

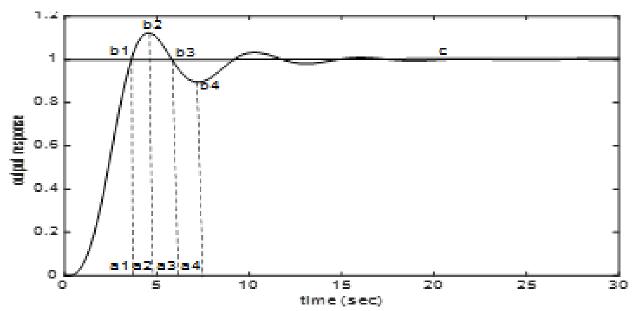

Figure 1a: Step response of the STFLPDC for Crane model.

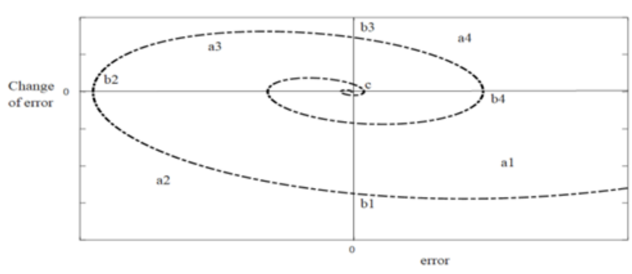

Figure 1b: The phase plane trajectory of the STFLPDC for Crane

Citation: Naskar I, Pal AK, Jana NK (2023) Variable Clustered Fuzzy Rules for Self-Tuning Scheme for Respiratory Distresses by Similarity and the Phase Plane Trajectory Concept. J Pulm Med Respir Res 9: 079.

Different conditions	Area
e>0 and Δe<0	a1
e<0 and Δe<0	a2
e<0 and Δe>0	a3
e>0 and Δe>0	a4
e>0 to e<0 and e<0	b1
e<0 to e>0 and Δe>0	b2
e<0 and Δe=0	b3
e>0 and Δe=0	b4
e=0 and Δe=0	C

Table 1: Response area mapping with the trajectory.

<table>
<tr><th>e/Δe</th><th>NB</th><th>NM</th><th>NS</th><th>NVS</th><th>PS</th><th>PM</th><th>PB</th></tr>
<tr><td>NB</td><td colspan="3" rowspan="3">a3</td><td rowspan="3">b3</td><td colspan="3" rowspan="3">a4</td></tr>
<tr><td>NM</td></tr>
<tr><td>NS</td></tr>
<tr><td>NVS</td><td colspan="3">b2</td><td>C</td><td colspan="3">b4</td></tr>
<tr><td>PS</td><td colspan="3" rowspan="3">a2</td><td rowspan="3">b1</td><td colspan="3" rowspan="3">a1</td></tr>
<tr><td>PM</td></tr>
<tr><td>PB</td></tr>
</table>

Table 2: Response area mapping with the trajectory plot.

e/Δe	NB	NM	NS	NVS	PS	PM	PB
NB				PSM			
NM				PSM			
NS				PSM			
NVS	PVS	PS	PSB	PSM	PM	PB	PVB
PS				PSM			
PM				PSM			
PB				PSM			

Table 3: Extracted 49 rules reduced to 13 rules by the phase plane trajectory.

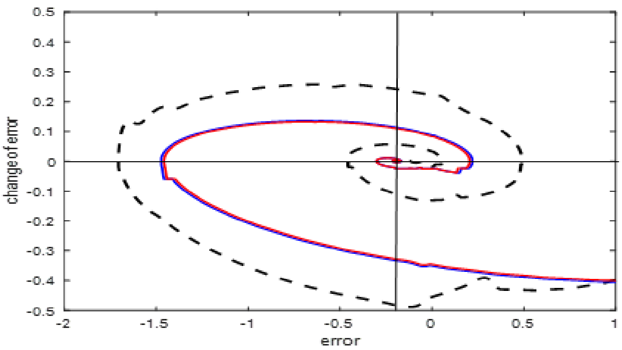

Figure 2: Phase Plane trajectory plot for inverted pendulum model 49 expert rules - - black, (49/21/16) extracted – blue, 13 rules by trajectory – red.

Different Demonstrated Model

Human Respiratory Model

The different sections of the human respiratory system are the nasal cavity (T_{FN}), trachea (T_{FT}), bronchi (T_{FB}), and alveoli (T_{FA}) [16, 17]. The individual transfer functions are derived from the circuit diagram of figure. 3 and with values presented in Table 4 as follows:

$$TF_N = \frac{1}{0.0027s^2+2.156s+1} \tag{8}$$

$$TF_T = \frac{1}{0.0037s^2+0.0054s+1} \tag{9}$$

$$TF_B = \frac{1}{0.0000144s^2+0.000402s+1} \tag{10}$$

$$TF_A = \frac{1}{0.0000000672s^2+0.000654s+1} \tag{11}$$

The resultant respiratory model T_{FM} is derived from the product of the individual models,

$$TF_M = TF_N * TF_T * TF_B * TF_A \tag{12}$$

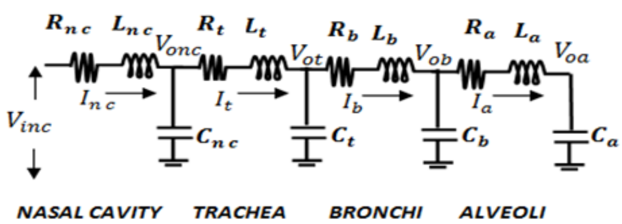

Figure 3: Electrical R, L, C model of the human respiratory system.

Different section of human respiratory system	R H_2O/Ltr/s	L H_2O/Ltr/s^2	C Ltr/cm of H_2O	RC	LC
NASAL CAVITY	16.332700	0.0200000000	0.1320	2.156000	0.00270000000
TRACHEA	0.086000	0.0059000000	0.0631	0.005400	0.00037000000
BRONCHI	0.008700	0.0002929000	0.0461	0.000402	0.00001440000
ALVEOLI	0.000550	0.0000000647	1.0396	0.000571	0.00000006720

Table 4. Different values of R, L, and C in different sections of respiratory tract.

Validation of the Respiratory Model

The derived model is validated in real-time by spirometry test, and the model transfer function (T_{FR}) as in equation (13) is derived using MATLAB System Identification Toolbox.

$$TF_R = \frac{0.0030984}{\{(1.7s+1)(0.109s+1)(0.001s+1)\}} \tag{13}$$

A comparison of T_{FR} and T_{FM} is presented in Figure 4 [16-18].

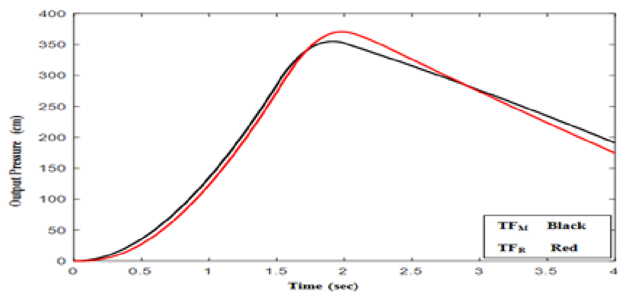

Figure 4: Comparison of the responses of the developed model and real model of respiratory system.

Design of Proposed STFLPDC

STFLPDC for human respiratory model

Because of obstructions in the respiratory pathway caused by human respiratory disorders like Bronchitis and Emphysema, less air enters the lungs than is necessary for proper respiration to occur. The result in adverse effects that have already occurred must be properly treated medically, and supplementary oxygen must be given in addition to this medicine in order to restore regular breathing [16,17].

In this study, expert and extracted rule-base for STFLPDC are provided to supply desired quantity of controlled oxygen to the patient. The developed respiratory model is used to test with the input as seen in figure. 5, and the outcomes of the proposed fuzzy model for STFLPDC using automatically extracted rules (49 rules), reduced extracted rules (29/14 rules), and 13 rules by trajectory approach are compared with expert knowledge-based 49 if-then rules.

The Input signal/ Normal breathing pattern

The breathing cycle in figure. 5 lasts a total of 4 seconds, with t_1 (inspiration time) equaling 1.5 seconds ($0 \leq t \leq t_1$) and t_2-t_1 (expiration time) equaling 2.5 seconds ($t_1 < t \leq t_2$).

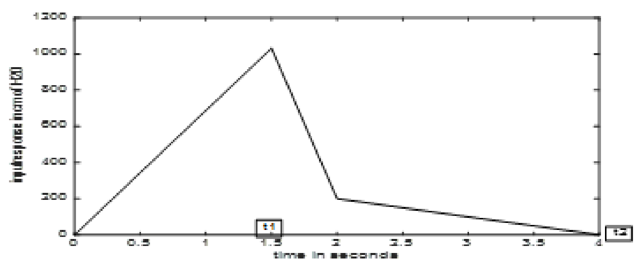

Figure 5: Normal breathing cycle.

Oxygen cylinder with valve model

The oxygen supply model to the patient developed from the electrical analogy drawn in figure. 6 as follows:

$$q = \frac{P_1 - P_2}{R} = C\frac{dP_2}{dt} \tag{14}$$

According to the patient's oxygen needs, P_1, P_2, q, R, and C in figure. 6 represent the input oxygen pressure, output oxygen pressure, oxygen flow rate, flow track resistance, and capacities of the system, respectively.

The oxygen supply system's transfer function can be deduced as follows:

$$TF_{cylinder} = \frac{P_2(S)}{P_1(S)} = \frac{1}{RCS+1} \tag{15}$$

To achieve the optimal fit value to build the $TF_{cylinder}$ model, the experiment is conducted with different set of R and C values and achieved the best result is at 0.25sec.

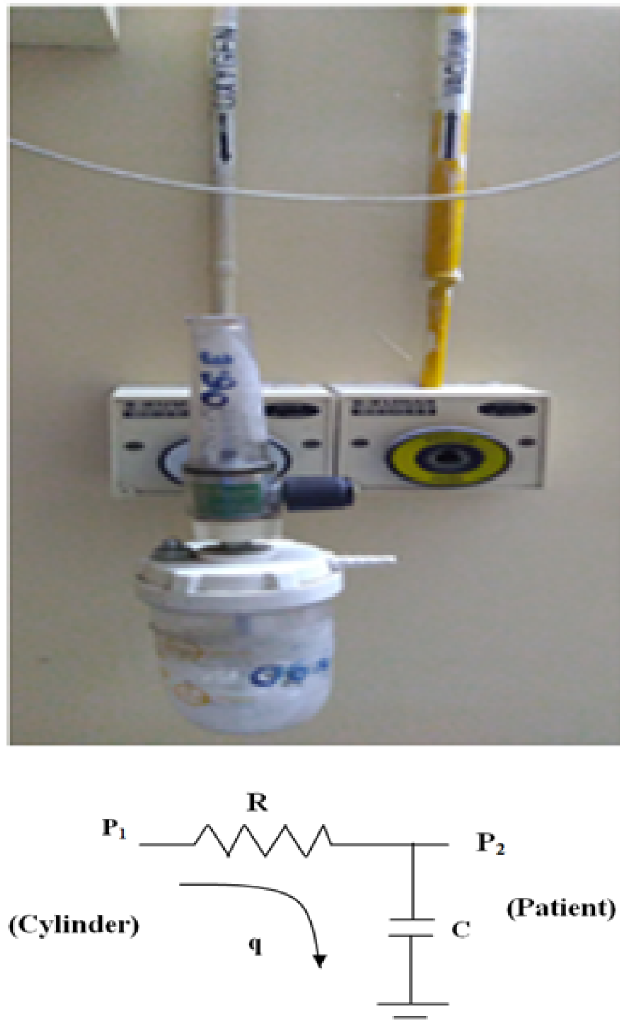

Figure 6: Oxygen supply electrical analogy model.

Development of the proposed STFLPDC Scheme

The STFLPDC is designed with 49 fuzzy if-then rules and 49 fuzzy gain rules exhibited in Table 5, this scheme is proposed here to auto-tune the model appeared in figure. 7. This scheme generates an additional automatic corrective gain signal 'β' at every instant, which coalesces with the FLPDC output 'u' and scaling factor 'G_u', to generate G_u*u*β to generate the tuned output for the required amount of O_2 supply to the patient.

e/Δe	NB	NM	NS	ZE	PS	PM	PB
NB	ZE	NS	NS	NM	NM	NM	NB
NM	PS	ZE	NS	NS	NS	NM	NM
NS	PS	PS	ZE	NS	NS	NM	NM
ZE	PS	PS	PS	ZE	NS	NS	NM
PS	PM	PM	PS	PS	ZE	NS	NS
PM	PM	PM	PM	PS	PS	ZE	NS
PB	PB	PB	PB	PM	PM	PS	ZE

(a) 49 Fuzzy Rules

e/Δe	NB	NM	NS	ZE	PS	PM	PB
NB	VB	VB	VB	B	SB	S	ZE
NM	VB	VB	B	B	MB	S	VS
NS	VB	MB	SB	MB	ZE	S	VS
ZE	S	SB	ZE	ZE	S	SB	S
PS	VS	S	ZE	MB	SB	MB	VB
PM	VS	S	MB	B	B	VB	VB
PB	ZE	S	SB	B	VB	VB	VB

(b) 49 Gain Rules

Table 5: Expert 49 rule matrix of FLPDC and 49 rule matrix of STFLPDC for respiratory model.

The automatic oxygen supply control scheme with STFLPDC for diseases like Bronchitis and Emphysema is depicted in figure. 7.

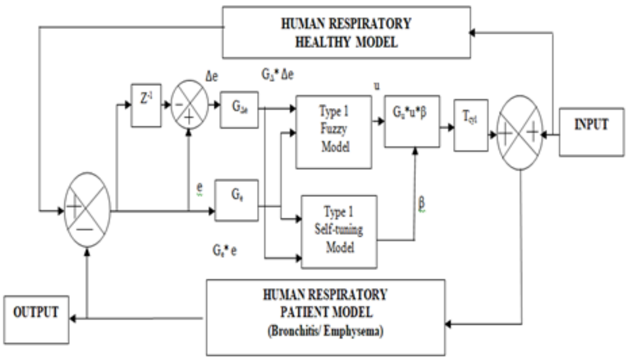

Figure 7: The proposed STFLPDC scheme.

The extracted (49/29/14) fuzzy rules by similarity analysis are shown in Tables 6-8 to build up the model of the self-tuning part of STFLPDC in the MATLAB Simulink environment. Another STFLPDC is designed by trajectory approach, where extracted 49 rules are reduced to 13 rules displayed in Table 3.

e/Δe	NB	NM	NS	PVS	PS	PM	PB
NB	PVS	PS	PSB	PSM	PM	PB	PVB
NM	PVS	PS	PSB	PSM	PM	PB	PVB
NS	PVS	PS	PSB	PSM	PM	PB	PVB
NVS	PVS	PS	PSB	PSM	PM	PB	PVB
PS	PVS	PS	PSB	PSM	PM	PB	PVB
PM	PVS	PS	PSB	PSM	PM	PB	PVB
PB	PVS	PS	PSB	PSM	PM	PB	PVB

Table 6: Extracted 49 rule matrix of STFLPDC developed respiratory model.

e/Δe	NB	NM	NS	PVS	PS	PM	PB
NB	PVS	PS	PSB	PSM			
NM	PVS	PS	PSB	PSM			
NS			PSB	PSM	PM	PB	
NVS			PSB	PSM	PM	PB	
PS			PSB	PSM	PM	PB	
PM			PSB	PSM	PM	PB	
PB			PSB	PSM	PM	PB	PVB

Table 7: Extracted 29 rule matrix of STFLPDC developed respiratory model.

e/Δe	NB	NM	NS	PVS	PS	PM	PB
NB	PVS	PS	PSB				
NM	PVS	PS	PSB				
NS				PSM			
NVS				PSM			
PS				PSM			
PM				PSM			
PB				PSM	PM	PB	PVB

Table 8. Extracted 14 rule matrix of stflpdc for developed respiratory model.

STFLPDC design for overhead crane

For the purpose of controlling an overhead crane, a dual control strategy employing a self-tuning PD technique is suggested [19,20], with one controlling position and the other controlling swing. To develop self-tuning FLPDC (STFLPDC), a span of ±1m and ±20° respectively for (*e*, Δ*e*, and *u/θ*) are considered for FLPDC section and for self-tuning part, the span of β is selected from [0m, +1m] and [0° (0c), +20° (0.349c)] 49 gain rules using Table 9 for position and angle control, respectively, while keeping *e,* Δe the same as shown in Figure 8 [21,22]. The gain rule base of STFLPDCs for position and angle controller are designed with 49/21/16 extracted gain rules in Tables 10-12.

e/Δe	NB	NM	NS	ZE	PS	PM	PB
NB	NB	NB	NB	NS	NS	NS	ZE
NM	NB	NM	NM	NM	NS	ZE	PS
NS	NB	NM	NS	NS	ZE	PS	PM
ZE	NB	NM	NS	ZE	PS	PM	PB
PS	NM	NS	ZE	PS	PS	PM	PB
PM	NS	ZE	PS	PM	PM	PM	PB
PB	ZE	PS	PS	PM	PB	PB	PB

(a) 49 Fuzzy Rules.

e/Δe	NB	NM	NS	ZE	PS	PM	PB
NB	VB	VB	VB	B	SB	S	ZE
NM	VB	VB	B	B	MB	S	VS
NS	VB	MB	SB	MB	ZE	S	VS
ZE	S	SB	ZE	ZE	S	SB	S
PS	VS	S	ZE	MB	SB	MB	VS
PM	VS	S	MB	B	B	VB	VB
PB	ZE	S	SB	B	VB	VB	VB

(b) 49 Gain Rules.

Table 9 : Expert 49 rule matrix of FLPDC and 49 gain rule matrix of STFLPDC of crane model for position and angle control

e/Δe	NB	NM	NS	NVS	PS	PM	PB
NB	PVS	PS	PSB	PSM	PM	PB	PVB
NM	PVS	PS	PSB	PSM	PM	PB	PVB
NS	PVS	PS	PSB	PSM	PM	PB	PVB
NVS	PVS	PS	PSB	PSM	PM	PB	PVB
PS	PVS	PS	PSB	PSM	PM	PB	PVB
PM	PVS	PS	PSB	PSM	PM	PB	PVB
PB	PVS	PS	PSB	PSM	PM	PB	PVB

e/Δe	NB	NM	NS	PVS	PS	PM	PB
NB	PVS	PS	PSB	PSM	PM	PB	PVB
NM	PVS	PS	PSB	PSM	PM	PB	PVB
NS	PVS	PS	PSB	PSM	PM	PB	PVB
PVS	PVS	PS	PSB	PSM	PM	PB	PVB
PS	PVS	PS	PSB	PSM	PM	PB	PVB
PM	PVS	PS	PSB	PSM	PM	PB	PVB
PB	PVS	PS	PSB	PSM	PM	PB	PVB

Table 10: Extracted 49 rule matrix of STFLPDC of crane model for position and angle control.

e/Δe	NB	NM	NS	NVS	PS	PM	PB
NB	PVS	PS	PSB				
NM	PVS	PS	PSB				
NS			PSB	PSM			
NVS			PSB	PSM			
PS			PSB	PSM			
PM			PSB	PSM	PM	PB	
PB			PSB	PSM	PM	PB	PVB

e/Δe	NB	NM	NS	PVS	PS	PM	PB
NB	PVS	PS	PSB				
NM	PVS	PS	PSB				
NS			PSB	PSM			
PVS			PSB	PSM			
PS			PSB	PSM			
PM			PSB	PSM	PM	PB	
PB			PSB	PSM	PM	PB	PVB

Table 11: Extracted 21 rule matrix of STFLPDC of crane model for position and angle control.

e/Δe	NB	NM	NS	NVS	PS	PM	PB
NB				PSM	PM		
NM				PSM	PM		
NS				PSM	PM		
NVS				PSM	PM		
PS				PSM	PM		
PM				PSM	PM		
PB				PSM	PM	PB	PVB

e/Δe	NB	NM	NS	PVS	PS	PM	PB
NB				PSM	PM		
NM				PSM	PM		
NS				PSM	PM		
PVS				PSM	PM		
PS				PSM	PM		
PM				PSM	PM		
PB				PSM	PM	PB	PVB

Table 12: Extracted 16 rule matrix of stflpdc for crane model for position and angle control.

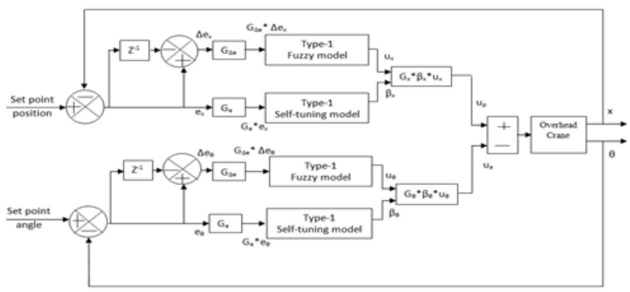

Figure 8: Block diagram of STFLPDC for overhead crane model.

Convergent Test

The rules are extracted by using FCM and this is validated through different validity indices mentioned in section 3 and the results are presented in Tables 13-14 below.

Cluster convergence test

The ratio M is expressed by the cost function

$$M = \frac{J(m+1) - J(m)}{J(m) - J(m-1)},$$

Where, m is iterations number.

The below Figures 9a-9c illustrates the FCM-based clusters are significantly converged as $M \leq 1$ for all e_k, Δe_k, β_k respectively.

Data set	PC	PE	XB	SC	DI
Error data	0.8707	0.0063	0.00075	0.7717	0.0014
Change of error data	0.8707	0.0063	0.00790	0.6628	0.0014
Output data	0.8862	0.0555	0.01520	0.9340	1.4831

Table 13: Different validity index for respiratory model.

	Data set	PC	PE	XB	SC	DI
Overhead crane: Position	Error data	0.8931	0.0190	0.0271	0.7635	0.0047
	Change of error data	0.8946	0.2020	0.0218	0.7406	0.0135
	Output data	0.8881	0.1664	0.0596	0.9437	1.2389
Overhead Crane: Angle	Error data	0.8910	0.0185	0.0263	0.6931	0.0014
	Change of error data	0.8906	0.0185	0.0263	0.7659	0.0014
	Output data	0.9343	0.0116	0.0674	0.9504	1.1328

Table 14: Different validity index for crane model.

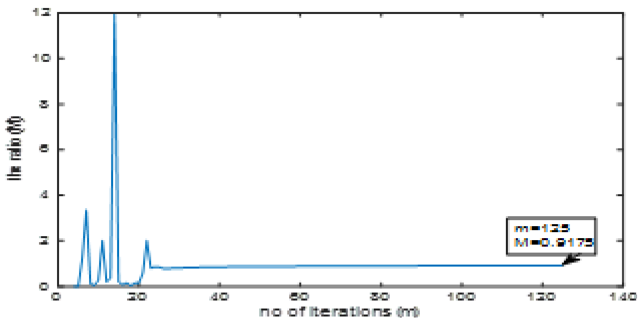

Figure 9a: Convergence test of the FCM cluster for ek.

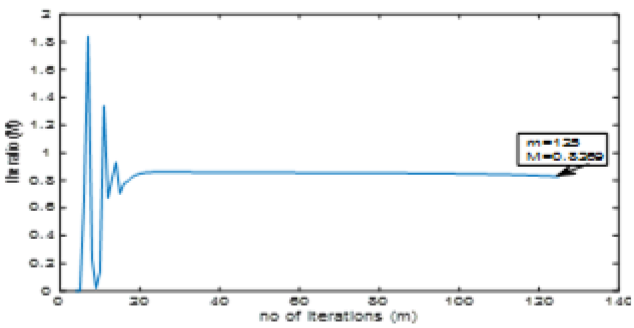

Figure 9b: Convergence test of the FCM cluster for Δek.

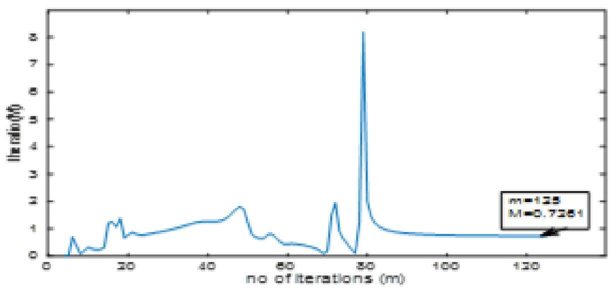

Figure 9c: Convergence test of the FCM cluster for βk.

Comparative Result Analysis

STFLPDC for respiratory model

In this study, the usefulness of the constructed self-tuning model STFLPDC with modifications of extracted gain rules in two different ways (similarity and trajectory) is demonstrated on the respiratory distress due to respiratory diseases, namely, Bronchitis and Emphysema, and tested with different oxygen cylinder models. The oxygen cylinder model 1/ (1+0.5*S) shows the better result in diseases like Bronchitis and Emphysema exhibited in Figure 11 and Figure 14 respectively. Now the proposed STFLPDC scheme is designed with automatically extracted gain rules (49), and subsequent reduction of rules by 59.18% (29), 28.57% (14), and 26.5% (13). The performance analysis of these controllers in the Bronchitis and Emphysema model is demonstrated in Figure 12 and Figure 15. The efficiency of the designed controllers is compared. The comparison with other controllers is shown in Figure 10 and Figure 13 for Bronchitis and Emphysema.

Bronchitis

The resistance of the bronchial section is increased by around 2000 times due to Bronchitis which impedes the O_2 intake and also slows down the respiratory process and as a result the bronchial model is changed to TF'_B.

$$TF'_B = 1/(0.0000144s^2 + 0.802s + 1) \tag{16}$$

Emphysema

The capacitance of the alveoli is increased by more than 5000 times due to long-term smoking cause's air to build up within these sacs f or Emphysema [23,24]. The diseased alveoli model is modified to TF'_A.

$$TF'_A = 1/(0.003s^2 + 3s + 1) \tag{17}$$

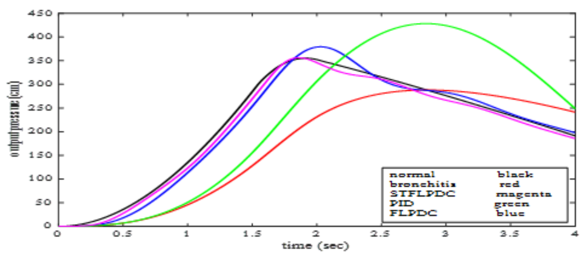

Figure 10: Study of different controllers on Bronchitis.

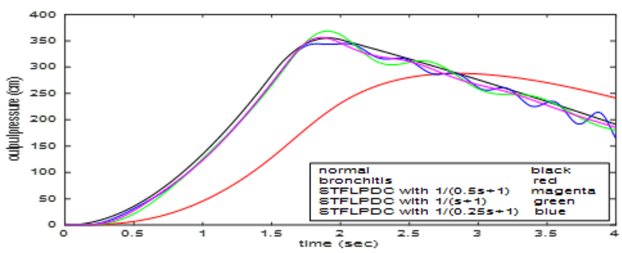

Figure 11: The effect of different combination of RC values for Bronchitis for the proposed STFLPDC.

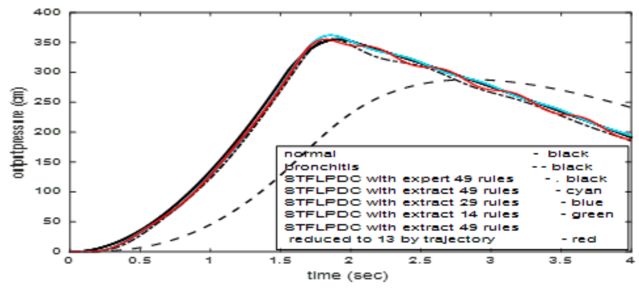

Figure 12: The effect of Bronchitis due to different extracted rules.

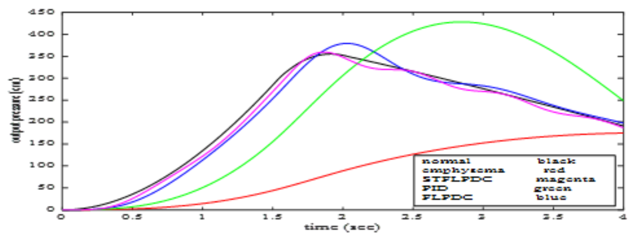

Figure 13: Study of different controllers on Emphysema.

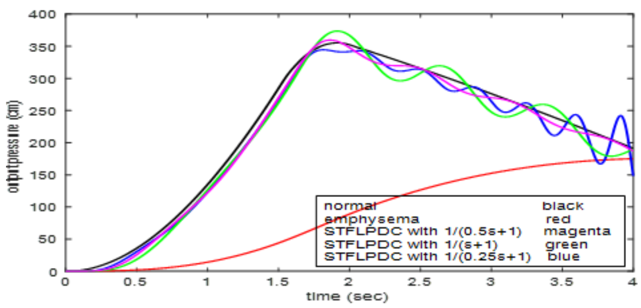

Figure 14: The effect of different combination of RC values for Emphysema for the proposed STFLPDC.

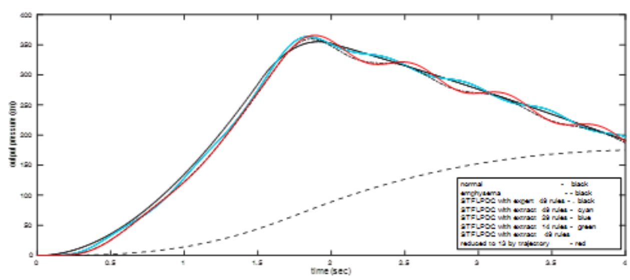

Figure 15: The effect of Emphysema due to different extracted rules.

The response due to STFLPDC for the developed respiratory model is done by calculating the correlation coefficient (R) (towards +1 (but less than +1) is an indicator of goodness).

$$R = \frac{cov(d_n, d_s)}{\sigma_n * \sigma_s} \tag{18}$$

Where, (d_n, σ_n) and (d_s, σ_s) are the data set and their standard deviation corresponds to the healthy patient model and responses due to different rules (expert, extracted, and trajectory) of proposed STFLPDC, FLPDC, and PID for respiratory model respectively. The effectiveness of the proposed controller for the respiratory models with extracted rules with the healthy patient for Bronchitis and Emphysema are presented by correlation coefficient and mean square error (MSE) as shown in Tables 15-16.

Controller	MSE with respect to healthy patient (Bronchitis)	Correlation coefficient with respect to healthy patient (Bronchitis)
STFLPDC (49 expert rules)	78.7638	0.9994
STFLPDC (49/29/14 extracted rules)	22.1460	0.9994
STFLPDC (13 trajectory rules)	28.2964	0.9994
FLPDC	273.7838	0.9927
PID	$9.4473*10^{03}$	0.8090

Table 15: Comparative study of different controllers for Bronchitis.

Controller	MSE with respect to healthy patient (Emphysema)	Correlation coefficient with respect to healthy patient (Emphysema)
STFLPDC (49 expert rules)	78.7638	0.9994
STFLPDC (49/29/14 extracted rules)	22.1460	0.9994
STFLPDC (13 trajectory rules)	28.2964	0.9994
FLPDC	273.7838	0.9927
PID	$9.4473*10^{03}$	0.8090

Table 16: Comparative study of different controllers for Emphysema

Real time application with STFLPDC for overhead crane model

Another STFLPDC [22] is designed with modifications of extracted gain rules Tables 18-20 and Table 21 by two different ways (similarity and trajectory) and demonstrated on a laboratory-based overhead crane system (Make: FEEDBACK, UK).

Due to the coupling between position and angle control under any loading/unloading condition in the actual plant, crane control is a challenging task [15,19]. The study takes a standard nonlinear crane model ("19" and "20") into consideration, and Table 17 displays the parameters used to design the overhead crane model as shown in Figure. 16 [25,26].

All the designed System responses show that the extraction and reduction (by both similarity and trajectory) of the rule base developed by both methods do not affect the system performance which ensures the success of the proposed rule extraction and reduction processes as shown in Figures. 10-20.

$$(M+m)\frac{d^2x}{dt^2}+K\frac{dx}{dt}=F_v+ml\sin\theta\left(\frac{d\theta}{dt}\right)^2-ml\cos\theta\frac{d^2\theta}{dt^2} \qquad (19)$$

$$\left(I+ml^2\right)\frac{d^2\theta}{dt^2}=mgl\sin\theta-ml\cos\theta\frac{d^2x}{dt^2} \qquad (20)$$

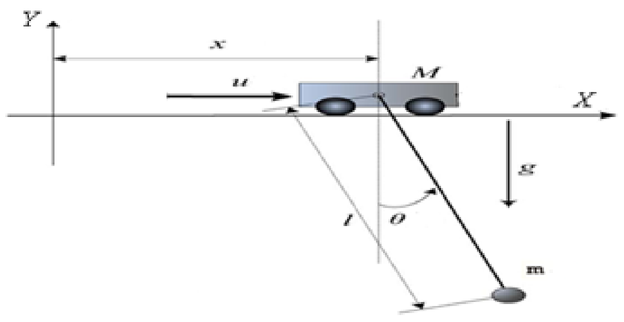

Figure 16: Pictorial view of the Overhead Crane.

m is the mass of the rod in kg	0.20
M is the mass of moving cart in kg	2.30
g is the acceleration due to gravity in m/s^2	9.81
l is the distance along the arm to the center of gravity in m	0.30
I is the moment of inertia of the pole in kgm^2	0.00990
K is the cart friction coefficient	0.00005

Table 17: Specification of overhead crane model.

e/Δe	NB	NM	NS	NVS	PS	PM	PB
NB	PVS	PS	PSB	PSM	PM	PB	PVB
NM	PVS	PS	PSB	PSM	PM	PB	PVB
NS	PVS	PS	PSB	PSM	PM	PB	PVB
NVS	PVS	PS	PSB	PSM	PM	PB	PVB
PS	PVS	PS	PSB	PSM	PM	PB	PVB
PM	PVS	PS	PSB	PSM	PM	PB	PVB
PB	PVS	PS	PSB	PSM	PM	PB	PVB

e/Δe	NB	NM	NS	PVS	PS	PM	PB
NB	PVS	PS	PSB	PSM	PM	PB	PVB
NM	PVS	PS	PSB	PSM	PM	PB	PVB
NS	PVS	PS	PSB	PSM	PM	PB	PVB
PVS	PVS	PS	PSB	PSM	PM	PB	PVB
PS	PVS	PS	PSB	PSM	PM	PB	PVB
PM	PVS	PS	PSB	PSM	PM	PB	PVB
PB	PVS	PS	PSB	PSM	PM	PB	PVB

Table 18: Extracted 49 gain rules.

e/Δe	NB	NM	NS	NVS	PS	PM	PB
NB	PVS	PS	PSB				
NM	PVS	PS	PSB				
NS			PSB	PSM			
NVS			PSB	PSM			
PS			PSB	PSM			
PM			PSB	PSM	PM	PB	
PB			PSB	PSM	PM	PB	PVB

e/Δe	NB	NM	NS	PVS	PS	PM	PB
NB	PVS	PS	PSB				
NM	PVS	PS	PSB				
NS			PSB	PSM			
PVS			PSB	PSM			
PS			PSB	PSM			
PM			PSB	PSM	PM	PB	
PB			PSB	PSM	PM	PB	PVB

Table 19: Extracted 21 gain rules.

e/Δe	NB	NM	NS	NVS	PS	PM	PB
NB				PSM	PM		
NM				PSM	PM		
NS				PSM	PM		
NVS				PSM	PM		
PS				PSM	PM		
PM				PSM	PM		
PB				PSM	PM	PB	PVB

e/Δe	NB	NM	NS	PVS	PS	PM	PB
NB				PSM	PM		
NM				PSM	PM		
NS				PSM	PM		
PVS				PSM	PM		
PS				PSM	PM		
PM				PSM	PM		
PB				PSM	PM	PB	PVB

Table 20: Extracted 16 gain rules.

e/Δe	NB	NM	NS	NVS	PS	PM	PB
NB				PSM			
NM				PSM			
NS				PSM			
NVS	PVS	PS	PSB	PSM	PM	PB	PVB
PS				PSM			
PM				PSM			
PB				PSM			

e/Δe	NB	NM	NS	PVS	PS	PM	PB
NB				PSM			
NM				PSM			
NS				PSM			
PVS	PVS	PS	PSB	PSM	PM	PB	PVB
PS				PSM			
PM				PSM			
PB				PSM			

Table 21: Extracted 13 gain rules by trajectory approach.

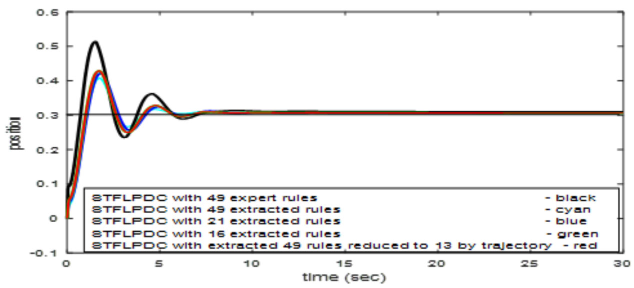

Figure 17: Study of STFLPDC (extracted 49/21/16 rules) to overhead crane position control and extracted 49 to13 rules by phase plane trajectory.

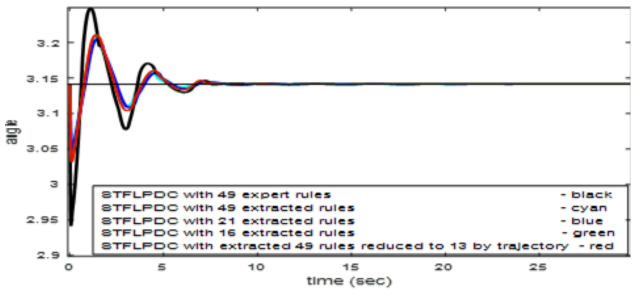

Figure 18: Study of STFLPDC (extracted 49/21/16 rules) for overhead crane angle control and extracted 49 to13 rules by phase plane trajectory.

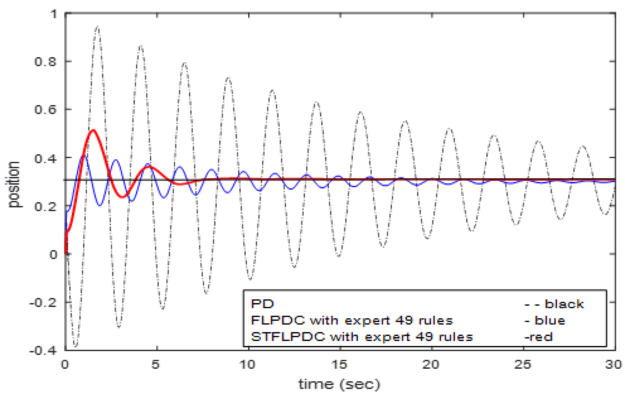

Figure 19: Study of different controllers for overhead crane position control.

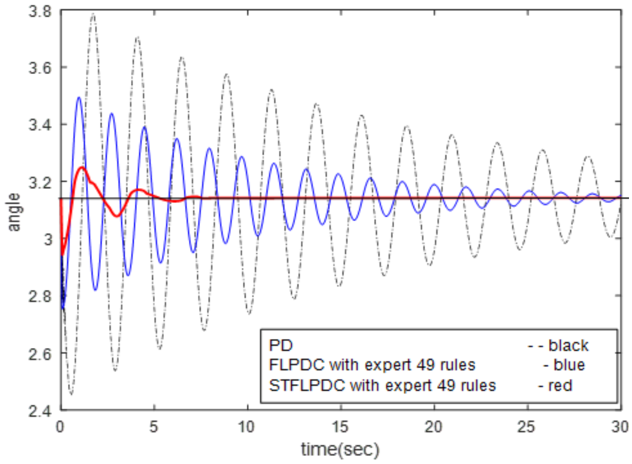

Figure 20: Study of different controllers for overhead crane angle control.

Controller	OS	T_s	IAE	ISE
Position control				
PD	63.7042	--	6.4078	2.1300
FLPDC	10.2791	--	0.7071	0.0367
STFLPDC(49 rules)	20.4617	7.8996	0.4773	0.0583
STFLPDC(49/21/16 extracted)	13.0125	7.5256	0.4233	0.0563
STFLPDC(13 trajectory)	13.0125	7.5256	0.4233	0.0563
Angle control				
PD	64.5341	--	6.3838	2.1163
FLPDC	35.3564	--	2.2245	0.3650
STFLPDC(49 rules)	10.7710	8.0501	0.2693	0.0207
STFLPDC (49/21/16 extracted)	8.9935	7.9221	0.2593	0.0197
STFLPDC(13 trajectory)	8.9935	7.9221	0.2593	0.0197

Table 22: Comparative study of different controllers for overhead crane.

Conclusion

A straightforward and efficient framework for obtaining the necessary response is provided by the proposed automatic extracted rule for self-tuning based fuzzy controllers. For self-tuning controllers, the automatic extracted/reduced fuzzy if-then rules using FCM and similarity analysis, and these extracted rules additionally reduced by phase plane trajectory are computationally effective and comprehensible. The varied rule bases of the designed controllers were successfully tested on the various systems. Various validity indices assess the separation and compactness of the cluster. The multiplier of the self-tuning controllers is varied by tuning the controllers with various numbers of extracted/reduced gain rule bases. It is evident that the proposed rule-base extraction technique for controllers performs successfully when comparing the results obtained by applying various other control schemes to the respiratory model to control oxygen supply regulation, and to the overhead crane to control position and swing to get desired response. The developed model has been validated using a real human respiratory system by spirometry test, and it has an accuracy of up to 95.63%. The proposed controller (STFLPDC) with variable extracted rules for bronchitis and emphysema disease responds better than expert rules, according to the correlation coefficient and mean square error metric (MSE) and also for crane model by comparing different performance indices. Experimental validation results show that the established rules for the various STFLPDC schemes have acceptable accuracy and good interpretation features.

References

1. Lee CC (1990) Fuzzy logic in control systems: fuzzy logic controller-Parts I, II. IEEE Trans. on System, Man, Cybern 20: 404-435.
2. Setnes M, Babuska R, Kaymak U, Lemke HRN (1998) Similarity measures in fuzzy rule base simplification. IEEE Trans. SMC-B 28: 376-386.
3. Wang L, Mendel JM (1992) Generating fuzzy rules by learning from examples. IEEE Trans. on System, Man, Cybern. 22: 1414-1427.
4. Dutu LC, Mauris G, Bolon P (2018) A fast and accurate rule-base generation method for Mamdani fuzzy systems. IEEE Trans. Fuzzy System 26: 715-733.
5. Kóczy LT, Botzheim J, Ruano AB, Chong A, Gedeon TD (2004) Fuzzy rule extraction from input/output data. Advances in Fuzzy Systems Applications and Theory. Machine Intelligence: 199-216.
6. Tarbosh, Qazwan A, Aydoğdu Ö, Farah N, Salh A, et al. (2020) Review and investigation of simplified rules fuzzy logic speed controller of high performance induction motor drives. IEEE digital object identifier.
7. Mohammed HR, Hussain ZM (2021) Hybrid Mamdani Fuzzy Rules and Convolutional Neural Networks for Analysis and Identification of Animal Images. Computation 9: 35.
8. Zhou X, Tan, Ding YZ, Liu Y (2021) Selecting Correct Methods to Extract Fuzzy Rules from Artificial Neural Network. Mathematics 9: 1164.
9. Hu YH, Zeo YC, Yang, Qu F (2011) A Cluster Validity Index for Fuzzy C-Means Clustering. International Conference on System Science, Engineering Design and Manufacturing Information 263-266.
10. Bezdek JC (1974) Cluster validity with fuzzy sets. J Cybernet 3: 58-72.
11. Mkhitaryan S, Wozniak MK, Giabbanelli P, Nápoles G, Vries De N, et al. (2022) FCMpy: a python module for constructing and analyzing fuzzy cognitive maps. Peer J Comput Sci 8:e1078.
12. Mohammed Al-Shammaa, and Maysam F Abbod (2022) Automatic Generation of Fuzzy Classification Rules from Data. Int J of Fuzzy Systems and Adv Appl 9: 63-68.
13. Marıa J, Romera L, Ballesteros M del MM, Gutierrez JG, Santos, JCR (2016) An Approach to Silhouette and Dunn Clustering Indices Applied to Big Data in Spark. Springer International Publishing Switzerland 2016, O. Luaces et al. (Eds.) pp 160-169.
14. Srikanth NV, Kumar DV (2004) Investigation of stability of fuzzy logic based power system stabilizers using phase-plane analysis. In Proc. Nat. Power Syst 408-413.
15. Park MS, Chwa D, Hong SK (2008) Antisway tracking control of overhead cranes with system uncertainties and actuator nonlinearity using an adaptive fuzzy sliding mode controls. IEEE Trans. on Industrial Electronics V-55: 3972-3984.
16. Naskar I, Pal AK, Jana NK (2023) Self-Regulating Adaptive Controller for Oxygen Support to Severe Respiratory Distress Patients and Human Respiratory System Modeling. MDPI-Diagnostics13: 967.
17. Naskar I, Pal AK (2022) Self Adaptive Fuzzy Controller for Supplementary Oxygen Supply to the Respiratory Distress Patients. J of Scient Research 14: 843-860.
18. Sharp JT, Henry Meadows JP, Sweany SK, Pietras RJ (1964) Total Respiratory Inertance and It's Gas and Tissue Components in Normal and Obese Men. Journal of Clinical Investigation, V43: 503-509.
19. Sorensen KL, Singhose W, Dickerson S (2007) A controller enabling precise positioning and sway reduction in bridge and grany crane. Control Engineering Practice 15: 825-837.
20. Pal AK, Mudi RK (2012) An adaptive fuzzy controller for an overhead crane. IEEE International Conference on Advanced Communication Control and Computing Technologies (ICACCCT) 300-304.
21. Mudi RK, Pal NR (1998) A self-tuning fuzzy PD controller. IETE Journal of Research Special Issue on Fuzzy Systems 44: 177-189.
22. Pal AK, Mudi RK, Maity RR De (2013) A non-fuzzy self-tuning scheme of PD-type FLC for an overhead crane Control. Advances in Intelligent Systems and Computing 199: 35-42.
23. Sethi S (1999) Infectious exacerbations of chronic bronchitis: diagnosis and management. Journal of Antimicrobial Chemotherapy 43: 97-105.
24. M El Garhy A, Ibrahim El Adawy M, Sawfta FO (2012) Design of fuzzy controller for supplying oxygen in sub-acute respiratory illnesses. International Journal of Computer Science Issues 9: 192-206.
25. Pal AK, Mudi RK, Dey C (2012) Rule Extraction through Self-Organizing Map for a Self-Tuning Fuzzy Logic Controller. Advanced Materials Research 403: 4957-4964.
26. Naskar I, Pal AK (2018) Type-2 Fuzzy Controller with Type-1 Tuning Scheme for Overhead Crane Control. Computational Intelligence, Communications, and Business Analytics 776: 567-576.

HERALD